Hindawi
International Journal of Distributed Sensor Networks
Volume 2024, Article ID 6670576, 11 pages
https://doi.org/10.1155/2024/6670576

Research Article

PHS: A Pulse Sequence Method Based on Hyperbolic Frequency Modulation for Speed Measurement

Tao Ping,[1] Caixia Song ,[2] Zhiguo Qi,[2] and Pengmin Xu[2]

[1]*Department of Science and Technology, Qingdao Agricultural University, Qingdao 266109, China*
[2]*College of Science and Information, Qingdao Agricultural University, Qingdao 266109, China*

Correspondence should be addressed to Caixia Song; cassiesong@qau.edu.cn

Received 1 February 2023; Revised 23 July 2023; Accepted 14 August 2023; Published 12 January 2024

Academic Editor: Saeed Olyaee

The channel in the marine environment is a time-varying and space-varying channel. Pulse-truncated continuous wave (PCW) speed measurement is often used in sonar, but the instability effect of PCW signal in the channel limits the effectiveness of speed measurement. Hyperbolic frequency modulation (HFM) signal is insensitive to Doppler; therefore, HFM signals are widely used in ranging and velocity measurement of sonar and radar. However, due to the filtering effect of the marine environment, the HFM signal of a single frequency band may cause excessive transmission loss, and the echo energy may be too weak to detect the target. Based on the analysis of the influence of speed on the distance measurement of HFM signal, a pulse sequence method based on HFM for speed measurement (PHS) is proposed, which uses HFM signals of different frequency bands and pulse widths in the pulse sequence to perform speed measurement. Extensive simulation results show that PHS method not only guarantees the speed measurement but also makes full use of the energy of the HFM sequence to improve the accuracy of the distance measurement. And PHS method is valuable to the practical application of engineering.

1. Introduction

The channel in the marine environment is a time-varying and space-varying channel [1]. The fading effect of the time-varying channel is divided into two situations:

(1) The frequency-domain fading effect caused by the frequency-varying characteristics of the channel, such as frequency dispersion and multipath

(2) Time-domain fading characteristics due to the time-varying characteristics of the channel, such as fluctuation and movement

In general, the so-called fading refers to the frequency-domain fading, and the time-domain fading generally refers to Doppler fluctuation. The unstable effect of pulse-truncated continuous wave (PCW) signal in the channel limits the effectiveness of speed measurement. Due to the Doppler invariant effect of HFM signal [2], in the underwater acoustic detection, the HFM signal is the most preferred [2–4]. However, some frequency bands have too much transmission loss in the channel, and a single HFM signal may not be able to detect the target.

In order to overcome the above limitations of speed measurement and ranging, a pulse sequence method based on HFM for speed measurement (PHS) is proposed, which uses HFM signals of different frequency bands and pulse widths in the sequence. Therefore, PHS method can not only measure the speed but also improve the accuracy of speed measurement and distance measurement. The main contributions of this paper are threefold:

(1) The PHS method employs HFM signals of different frequency bands and pulse widths in the sequence. And then, there are some problems under marine environments; for example, due to excessive propagation loss in certain frequency bands, the echo energy is insufficient and cannot effectively detect the target, which can be thus avoided

(2) Different combinations of HFM signals in the sequence can be coherent accumulation, and the signal-to-noise ratio (SNR) of the signals is improved. Therefore, the signals are more obvious

(3) The HFM signals in the sequence can mutually calculate the speed and distance of the target, reducing the calculation error caused by a single signal calculation, and the accuracy of velocity measurement and ranging is thus greatly improved

In Peng et al. [5], a joint linear frequency modulation and hyperbolic frequency modulation approach for speed measurement (JLHS) is proposed. The JLHS method uses the same pulse width and frequency band of positive and negative frequency modulation signals (LFM+HFM) for speed measurement and ranging. On the other hand, two signal modulation methods are required to be opposite in JLHS. Compared with JLHS, in the PHS method, the HFM signals are only not to be completely consistent, which relaxes the requirements of bandwidth and pulse width and makes it more suitable for general conditions. On the other hand, since the tolerance of LFM to moving targets is far less than that of HFM, when the target speed is too high, LFM will have no peak output after matched filtering, and thus, JLHS cannot realize ranging and speed measurement.

In our previous work [6], a speed measurement method of combined HFM signals (SCH) is proposed, which employs positive and negative HFM signals for speed measurement and ranging. It is well known that the channel in the marine environment is a time-varying and space-varying channel. Due to the filtering effect of the marine environment, the HFM signal of a single frequency band may cause excessive propagation loss, and the echo energy may be too weak to detect the target. Compared with SCH, in the PHS method, the HFM signals in pulse sequence adopt different frequency bands, and the more pulse forms in the pulse sequence, the easier it is for more echoes to return. Therefore, HFM pulse sequence signals are more conducive to engineering use.

2. Related Works

A new polyphase pulse compression code is proposed by Yang and Sarkar [7], which is derived from the stepwise approximation of the phase curve of a hyperbolic FM-chirp signal. And they solve the problem of relatively high sidelobe levels without Doppler effect by employing appropriate window functions. In multiuser communication systems (e.g., such as multiuser radar and sonar and multiple-access spread-spectrum communication systems), there has always been a problem, that is, the problem of frequency-hopping codes, which was successfully solved by Maric and Titlebaum [8]. The construction of a new family of frequency-hopping codes is given, and it is shown that hyperbolic frequency-hopping codes have almost ideal properties and can be used in two types of systems. To address the problem of conveniently handling the received energy while transmitting and receiving modulated energy, Whyland ([9]) proposed the use of Doppler-insensitive waveforms to modulate energy pulses or subpulses to probe a defined environment. For the sonar velocity measurement problem, many scholars are currently conducting research. Shao et al. [10] proposed the use of HFM+PCW-combined signal at the Western Acoustics Conference. The HFM signal is used for ranging, and the PCW is used for velocity measurement. The PCW signal cannot consistently and effectively contact the target due to its unstable operation in the sound field. Therefore, PCW can achieve speed measurement in echoes with high SNR. When the SNR does not meet the requirements slightly, PCW will cause a large speed measurement error. Peng et al. [5] used HFM and LFM signals with the same frequency band and the same pulse width for speed measurement. This method takes advantage of the advantages of HFM and LFM at the same time, but it needs to meet certain requirements for SNR. When the SNR is too low, LFM has no peak output, resulting in failure of distance and speed calculation. HFM waveform has inherent Doppler invariant characteristics. Based on this, Meng et al. [4] worked out the constraints on HFM parameters in order to better reduce the multiple-access interference at the transmission end. The multipath and scaled underwater channel effects are reduced due to additional limitations on the frequency modulation rate. After extensive experimental comparisons of the proposed signaling scheme with HFM-based CDMA schemes, the improved performance of the new scheme is demonstrated. In Gini and Giannakis [11], the parameter estimation problem of the combination of polynomial phase signal and HFM is well solved. In Xin [12], an improved preamble waveform UMD-HFM is proposed. On the basis of the UD-HFM signal, a blank interval is added to resist the delay expansion and Doppler delay of the multipath channel to avoid waveform stacking shown, but the use and variation of blanking intervals are not indicated. In order to overcome the multipath effect and the strong Doppler effect of the shallow sea, the HFM-SS spread-spectrum modulation is used for communication [13], and the Doppler invariance of HFM is fully utilized. However, this paper only considers a single HFM and does not consider using the relationship between the HFMs in spread-spectrum modulation to solve the Doppler. During the communication process, UD-HFM uses the positive and negative HFM as the preamble signal to estimate the Doppler velocity [14]. In order to avoid waveform superposition, the mute time is increased. This method defaults to the invariance of the mute time in the process of calculating the Doppler factor, but the mute time is changed at this time. On the other hand, the UD-HFM signal in this paper requires that the two HFMs are signals of the same frequency band and the same pulse width, which is a waste of frequency band utilization. At the same time, it is not conducive to overcoming the frequency selection characteristics of ocean channels. Liu et al. [15] presented mathematical formulations for multipath propagation model and the corrupted echoes. The impact of the multipath propagation on target detection is then analyzed. In addition, in order to remove the ghost targets, a simple but effective algorithm is proposed. Numerical simulation results show the satisfactory performance. In Murray [16], an extended matching filter is introduced into the HFM waveform in active sonar systems and provides an accurate closed-form solution to Doppler bias in arrival time estimates. The solution is suitable for broadband and narrowband HFM signals.

3. Ranging and Speed Measurement Based on PHS Method

According to the properties of the Fourier transform, the convolution of two signals in the time domain is equivalent to the multiplication of their FFT in the frequency domain. Convolution in the time domain can also realize the velocity measurement function. However, the convolution calculation in the time domain is more complex. This is because the convolution calculation in the time domain requires the signal to multiply and add different shift points, which requires a large amount of computation and more hardware memory, while the FFT multiplication in the frequency domain is simple to calculate and easier to implement. Therefore, in this paper, we use HFM signals of different frequency bands and pulse widths in the sequence to realize speed measurement.

Figure 1 shows the working process of the PHS method. When active sonar works, the transmitting system transmits several acoustic signals with specific information into the seawater separately, such as HFM signal 1 and HFM signal 2, which are called the transmitting signals. When the transmitting signals travel in seawater and meet targets, the echo signals will be generated. The echo signals propagate in the sea water according to the law of propagation and reach the hydrophone, which convert the acoustic signals into electrical signals. The electrical signals are processed by the signals (matching filtering and obtaining the peak time of each HFM signal, designing the function model and calculating, and coherent integration MTD operating between pulse trains) to obtain the distance and speed of the target.

4. The Principle of Velocity Measurement by Pulse Sequence Signals

Let T denote the pulse width of the HFM signal, f_0 denote the starting frequency of the HFM signal, f_1 denote the ending frequency of the HFM signal, and $s_s(t)$ denote the HFM transmitting signal changing over time. Then, $s_s(t)$ can be calculated by

$$s_s(t) = \begin{cases} \cos\left(-2\pi k \ln\left(1 - \frac{t}{t'}\right)\right), & -\frac{T}{2} \le t \le \frac{T}{2}, \\ 0, & \text{otherwise}, \end{cases} \tag{1}$$

where $t' = (T/2) \times ((f_1 + f_0)/(f_1 - f_0))$ and $k = (T f_0 f_1)/(f_1 - f_0)$.

Let $f_s(t)$ denote the instantaneous frequency of HFM transmitting signal, and it can be expressed as the derivative of the signal phase with respect to time divided by 2π. We have [6]

$$f_s(t) = \frac{k}{t' - t}. \tag{2}$$

The velocity of the target is denoted by v. When the target is moving at a speed of v, the relative motion between the sonar and the target results in a pulse width of T for the transmitted signal. At the receiving point, the transmitted signal becomes a signal with pulse width of T/η. Therefore, the pulse width of the echo is linearly compressed or stretched η times. And we have [6]

$$\eta = \frac{c + v}{c - v}, \tag{3}$$

where c represents the speed of sound in water and $c =$ 1500 m/s.

Let $s_r(t)$ represent the received echo signal. Due to the radial movement between the target and the sonar platform, $s_r(t)$ can be calculated as

$$s_r(t) = \begin{cases} \cos\left(-2\pi k \ln\left(1 - \frac{\eta t}{t'}\right)\right), & -\frac{T}{2} \le t \le \frac{T}{2}, \\ 0, & \text{otherwise}. \end{cases} \tag{4}$$

Let $f_r(t)$ represent the instantaneous frequency of the received echo. According to Equation (4), $f_r(t)$ can be expressed as

$$f_r(t) = \frac{\eta k}{t' - \eta t}. \tag{5}$$

Since the HFM signal is insensitive to Doppler, the HFM signal has the characteristic of Doppler invariance [2]. Moreover, the change rule of the instantaneous frequency of the received signal remains unchanged, except that the instantaneous frequency $f_s(t)$ of the original signal is shifted by a time t_0, where t_0 represents matched filter delay caused by target Doppler. We have [6]

$$f_s(t - t_0) = f_r(t). \tag{6}$$

Based on Equation (2), Equation (5), and Equation (6), t_0 can be computed as

$$t_0 = \frac{1 - \eta}{\eta} t'. \tag{7}$$

In practical applications, the arrival time of the target is unknown, and the Doppler-induced delay t_0 and the uncertainty of the arrival time of the target coexist, resulting in a single HFM signal unable to obtain a resolvable Doppler-induced delay t_0, as shown in Figure 2.

Frequency band and pulse width are the two key elements to consider when HFM signals are used for object detection. In order to obtain the delay difference and delay ratio after matched filtering, two HFM pulse signals (HFM

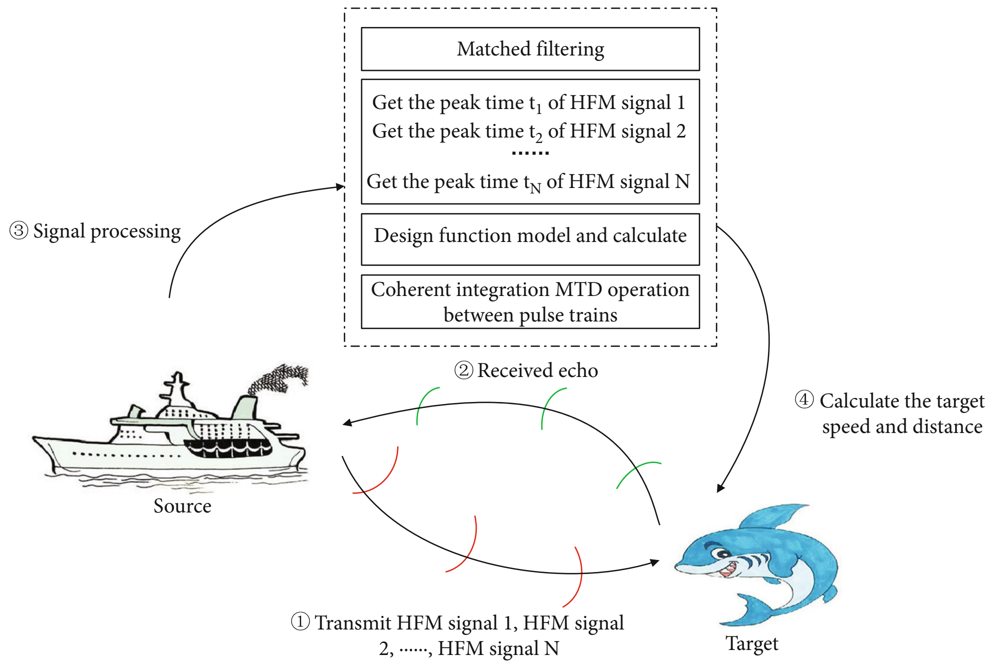

Figure 1: The work processing of the PHS method.

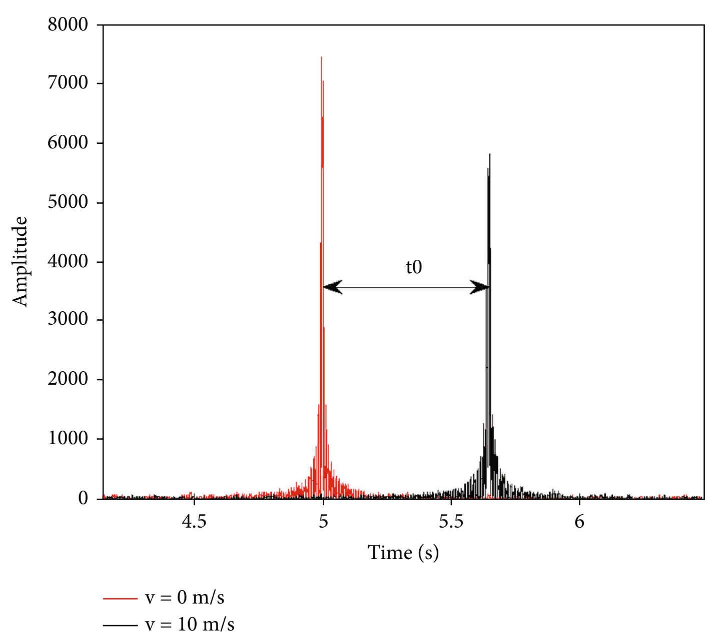

Figure 2: The delay after matched filtering caused by velocity.

pulse signal 1 and HFM pulse signal 2) in the pulse sequence are adopted.

Note: in this paper, HFM signal represents HFM pulse signal.

HFM signal 1: the starting frequency is denoted by f_{10}, the ending frequency is denoted by f_{11}, and the pulse width is denoted by T_1.

HFM signal 2: the starting frequency is denoted by f_{20}, the ending frequency is denoted by f_{21}, and the pulse width is denoted by T_2.

For a moving target, the time delay t_{d1} of HFM signal 1 can be computed as Equation (8). On the other hand, the time delay t_{d2} of HFM signal 2 can be computed as Equation (9).

$$t_{d1} = \frac{1-\eta}{\eta} t_1', \tag{8}$$

$$t_{d2} = \frac{1-\eta}{\eta} t_2', \tag{9}$$

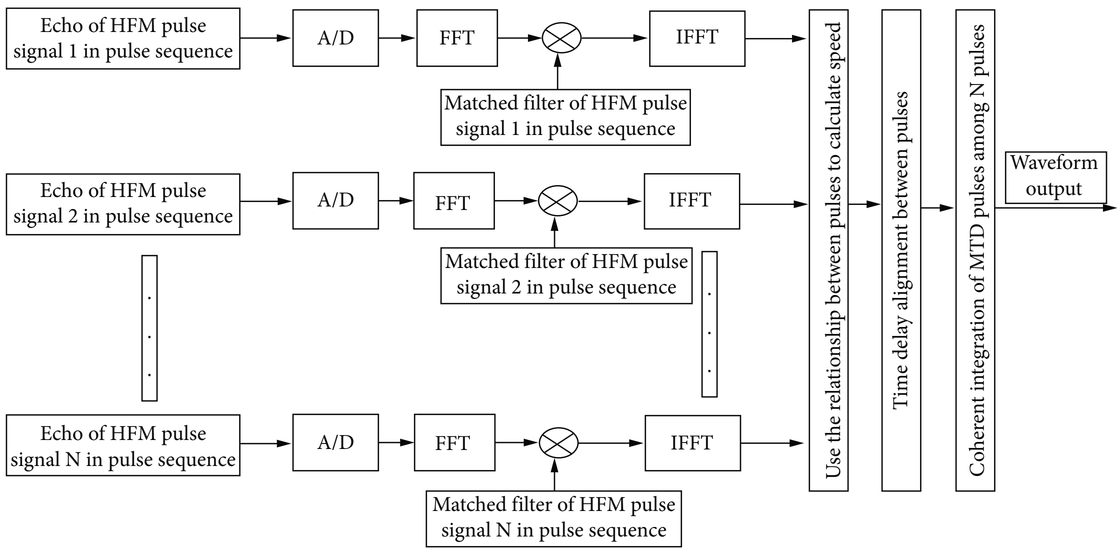

Figure 3: Signal processing diagram of pulse sequences.

where

$$\begin{cases} t_1' = \dfrac{T_1}{2} \times \dfrac{f_{11} + f_{10}}{f_{11} - f_{10}}, \\ t_2' = \dfrac{T_2}{2} \times \dfrac{f_{21} + f_{20}}{f_{21} - f_{20}}. \end{cases} \quad (10)$$

Dividing Equation (8) by Equation (9), we can obtain the ratio as follows:

$$\frac{t_{d1}}{t_{d2}} = \frac{t_1'}{t_2'}. \quad (11)$$

Now, let us derive the formulas of both ranging and speed measurement. Assume that the velocity v of the target towards the sonar system is positive. Two combined HFM signals in pulse sequence, HFM signal 1 and HFM signal 2, are transmitted. Let t_1 and t_2 represent the time of maximum matched filter of HFM signal 1 and the time of maximum matched filter of HFM signal 2, respectively. We have

$$t_1 = \frac{2R}{c} + t_{d1}, \quad (12)$$

$$t_2 = \frac{2R}{c} + t_{d2}. \quad (13)$$

According to the above two equations (Equations (12) and (13)), the distance R between the sonar and the target can be computed as

$$R = \frac{1}{2} c \left(\frac{t_1 - \left(t_1'/t_2'\right) t_2}{1 - \left(t_1'/t_2'\right)} \right). \quad (14)$$

Another form of R is

$$R = \frac{1}{2} \times c \times \tau, \quad (15)$$

where arrival time of the pulse is denoted by τ.

According to Equations (14) and (15), τ is obtained.

$$\tau = \frac{t_1 t_2' - t_1' t_2}{t_2' - t_1'}. \quad (16)$$

And then, based on Equation (12) and Equation (16), t_{d1} can be computed by

$$t_{d1} = t_1 - \tau. \quad (17)$$

According to Equations (3), (16), and (17), the target speed v can be obtained.

$$v = -\frac{xc}{x + 2}. \quad (18)$$

where

$$x = \left(t_1 - \frac{t_1 - \left(t_1'/t_2'\right) t_2}{1 - \left(t_1'/t_2'\right)} \right) \frac{1}{t'_1}. \quad (19)$$

The ideal transmission channel is an infinite space composed of lossless and uniform medium, and during the propagation process, the signal cannot have any distortion. However, it is well known that the seawater medium space is a lossy heterogeneous medium space. In addition to general absorption and diffusion, the signal in sea water is also affected by multipath effect, channel time-varying and fluctuation effect, which result in the broadening of the echo and the difficulty in distinguishing the echo position of the

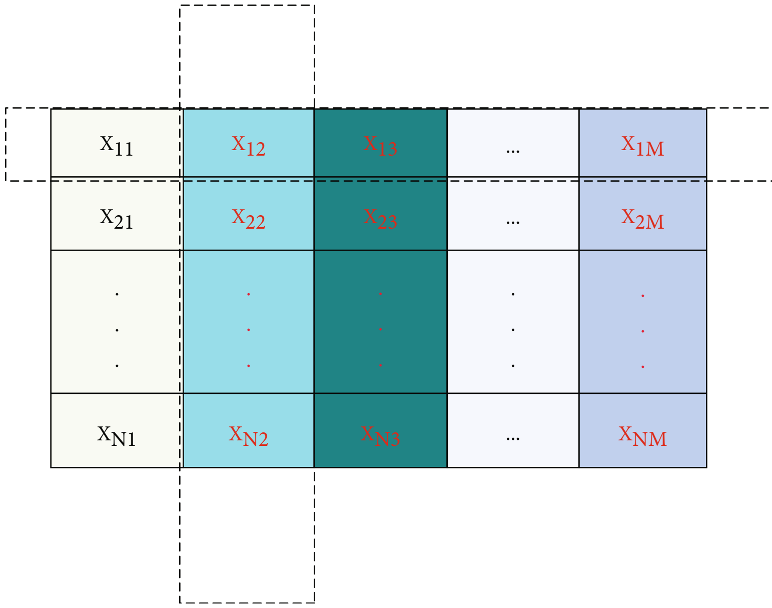

Figure 4: Diagram of coherent integration.

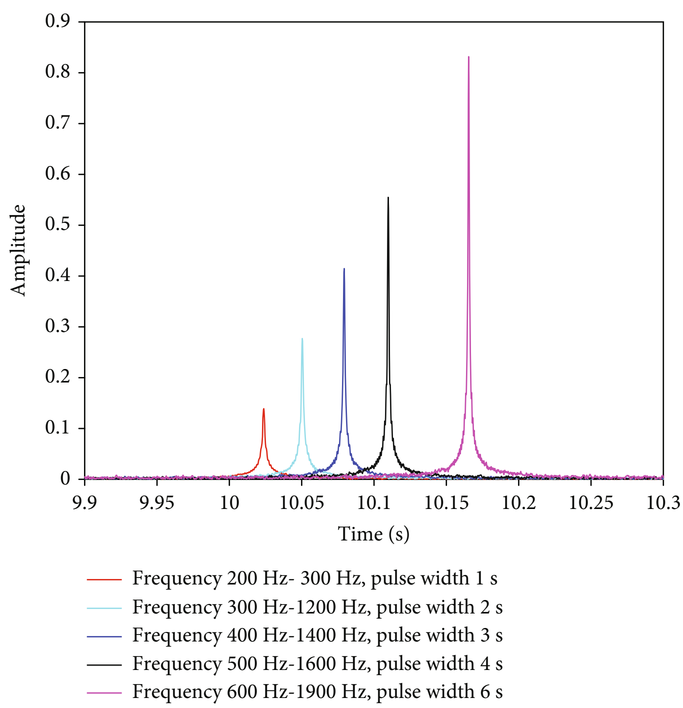

Figure 5: Single HFM signal detection under simulation environment 1.

combined echo signal. In order to achieve accurate speed measurement, we employ multiple HFM signals in pulse sequence, and the HFM signals adopt different frequency bands, and the more pulse forms in the pulse sequence, the easier it is for more echoes to return. Therefore, the signals are more obvious. Based on the above analysis, we can see that the HFM pulse sequence signals are more conducive to engineering use.

5. Moving Target Detection (MTD) between Pulse Sequences

The moving target detection (MTD) processing in pulse sequence is shown in Figure 3. It is assumed that the number of peak output of different HFM signals in the pulse sequence is N. Using the N peak outputs of pulse sequence to perform calculation in pairs, the speed and the

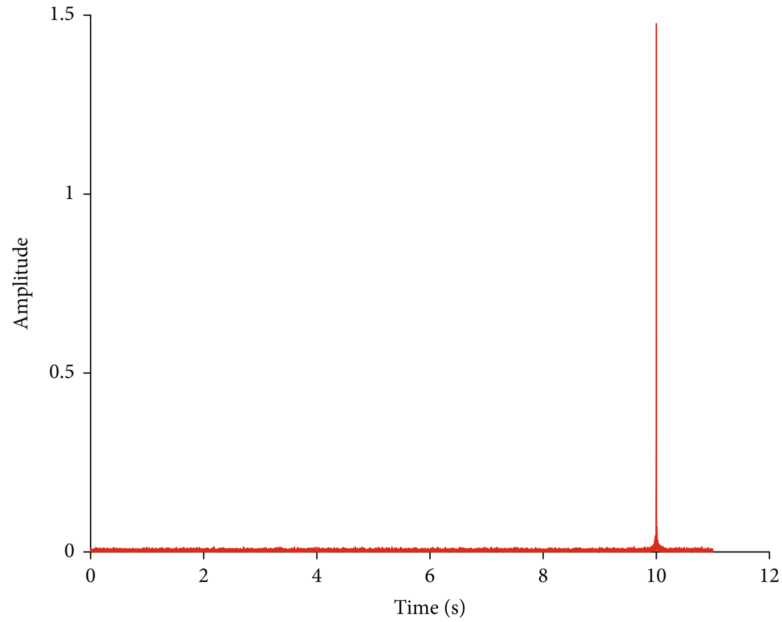

Figure 6: Pulse sequence method based on HFM signal under simulation environment 1.

Table 1: For simulated environment 1: comparison of simulation results.

(a)

Echo time of single signal (s)					Ranging of single signal (km)					Ranging of PHS (km)	Speed of PHS (m/s)
HFM signal 1	HFM signal 2	HFM signal 3	HFM signal 4	HFM signal 5	HFM signal 1	HFM signal 2	HFM signal 3	HFM signal 4	HFM signal 5		
10.0236	10.0502	10.0792	10.1096	10.1652	7.5177	7.53765	7.5594	7.5822	7.6239	7.5	13.9914

(b)

Ranging error of PHS	Speed measurement error of PHS	Ranging error of single signal					Range accuracy improvement ratio compared to				
		HFM signal 1	HFM signal 2	HFM signal 3	HFM signal 4	HFM signal 5	HFM signal 1	HFM signal 2	HFM signal 3	HFM signal 4	HFM signal 5
0%	0.061429%	0.236%	0.502%	0.792%	1.096%	1.652%	100%	100%	100%	100%	100%

corresponding distance can be obtained. Therefore, the total number of speeds and corresponding distances of the target is C_N^2. However, since the ocean environment changes in time and space, the ocean channel is equivalent to a filter. The signal in some frequency bands has too much propagation loss, resulting in too low signal energy in the echo that cannot be effectively detected. On the other hand, although some echoes can be detected, the SNR is too low, and the noise leads to an error between the arrival time of the signal and the actual arrival time of the echo of the target. Therefore, the peak outputs with high SNR are selected in the pulse sequence to calculate the speed and distance, which will make the calculation results more accurate.

6. Processing between Pulse Sequences

6.1. Incoherent Integration. Modelling the received echo sequence, that is, removing the phase information, for cross-period addition is called noncoherent integration or integration after detection. Generally speaking, since noncoherent integration does not utilize phase information, its detection performance is inferior to that of coherent integration. The difference between coherent integration and noncoherent integration is called detection loss. The detection loss is related to the SNR of the input. The larger the SNR is, the smaller the detection loss is. To take an extreme example, when the SNR is infinite (i.e., the noise is zero), the result of noncoherent integration is the same as that of coherent integration, and then, the detection loss is zero. In fact, as long as the input SNR is greater than 1, the detection loss is relatively small, and then, the coherent integration can be replaced by noncoherent integration. On the one hand, noncoherent integration is relatively simple to implement in engineering, and there is no strict coherence requirement for the system. On the other hand, for most moving targets, the fluctuation of the echo signals will

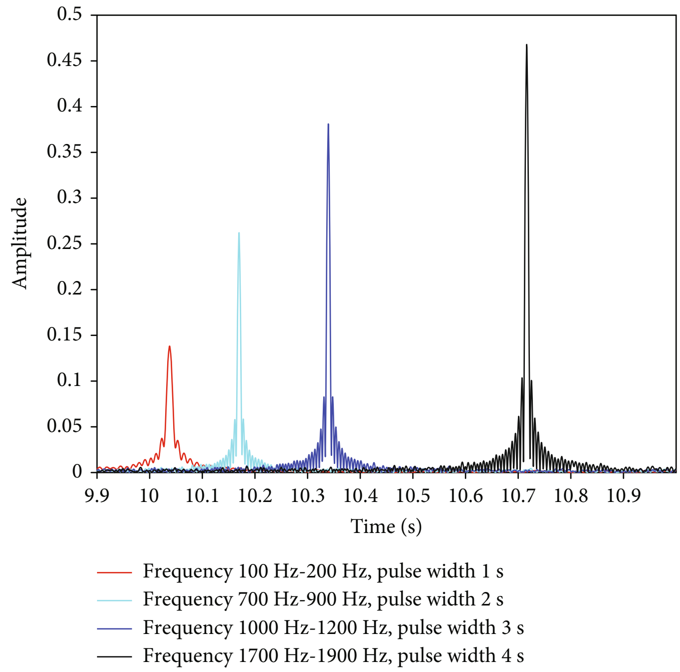

Figure 7: Single HFM signal detection under simulation environment 2.

obviously destroy the phase coherence of the adjacent echo signals. Therefore, even if the radar system has good coherence, it is difficult to obtain ideal coherent integration for undulating echoes. Therefore, although the SNR of noncoherent integration is not as good as coherent integration, noncoherent integration is often used in many cases [17]. However, noncoherent integration does not make full use of the phase of the signal, and then, the gain ratio is smaller than that of coherent integration.

6.2. Coherent Integration. Using the velocity and the corresponding distance, the echo signals are transplanted to the same starting point to carry out coherent integration MTD operation. And the coherent integration MTD is an integration method to improve the SNR of the target, which is generally performed on the complex envelope of the intermediate frequency signal or the zero intermediate frequency signal. Moreover, the coherent integration MTD retains the phase relationship between the received pulses and can increase the accumulated signal energy. That is, coherent integration utilizes the phase information of all the pulses. It is assumed that the total number of pulse echoes received during a pulse accumulation period is N, and each pulse cycle is divided into M distance gates. Discrete sampling is carried out for N pulse echoes, respectively, and let x_{nm} represent the sampling data on the mth distance gate of the nth pulse echo. Then, the sampling data of N pulse echo sequences can be expressed as a data of $N * M$ dimension, as shown in Figure 4. The signal amplitude can be greatly increased by the following: (1) M distance gates are fast time steps, and pulse compression processing is carried out. (2) N pulse echoes are slow time steps, and coherent pulse integration MTD is performed. The distance and velocity obtained

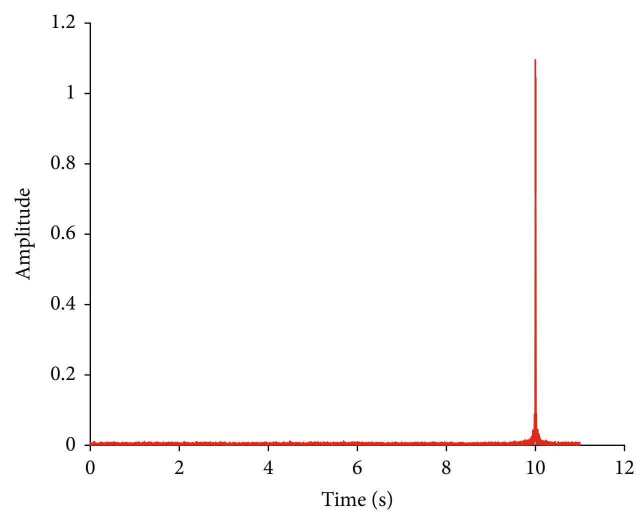

Figure 8: Pulse sequence method based on HFM signal under simulation environment 2.

in Section 4 are used to remove the signal delay in the pulse sequences, which is caused by the Doppler movement of the target. After the echo signals are rearranged, MTD operation is carried out, and then, a signal gain of N times can be achieved.

The time complexity of the proposed PHS method will be given by the following analysis. It is assumed that the number of the HFM signals in the pulse sequences is N. Since echo signal in each pulse sequence needs to be matched and filtered separately, the time complexity is $O(N)$. On the other hand, during space beamforming, due to different frequency bands in the sequences, separate

Table 2: For simulated environment 2: comparison of simulation results.

(a)

Echo time of single signal (s)				Ranging of single signal (km)				Ranging of PHS (km)	Speed of PHS (m/s)
HFM signal 1	HFM signal 2	HFM signal 3	HFM signal 4	HFM signal 1	HFM signal 2	HFM signal 3	HFM signal 4		
10.0376	10.1696	10.3392	10.7160	7.5282	7.6272	7.7544	8.037	7.5	14.0019

(b)

Ranging error of PHS	Speed measurement error of PHS	Ranging error of single signal				Range accuracy improvement ratio compared to			
		HFM signal 1	HFM signal 2	HFM signal 3	HFM signal 4	HFM signal 1	HFM signal 2	HFM signal 3	HFM signal 4
0%	0.013571429%	0.376%	1.696%	3.392%	7.16%	100%	100%	100%	100%

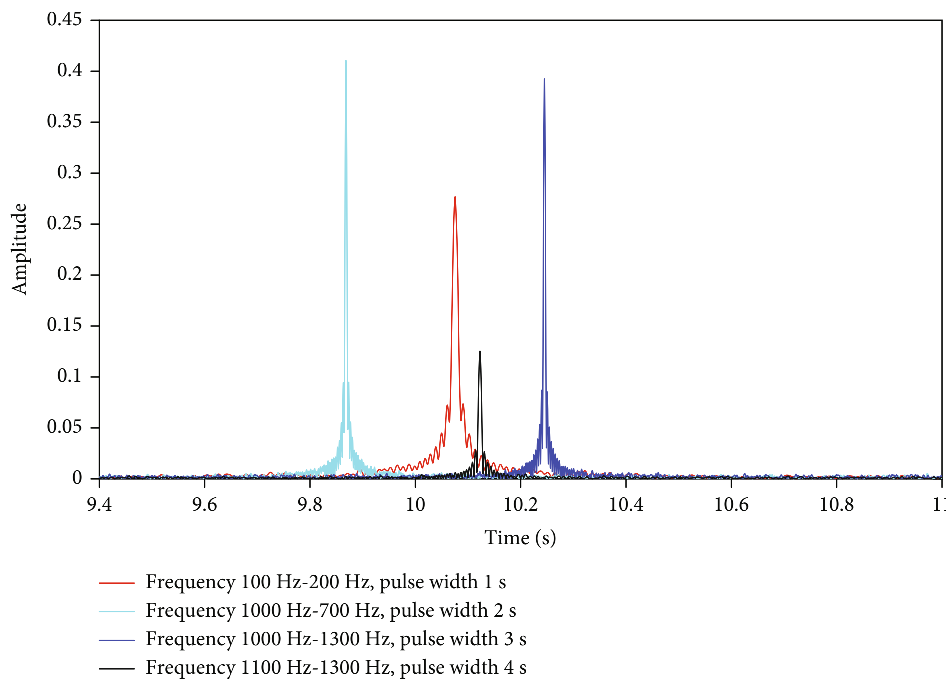

Figure 9: Single HFM signal detection under simulation environment 3.

beamforming is required, so the space complexity is $O(N)$. When the signal frequency bands in the sequences are the same and the pulse widths are different, the beamforming can only be done once, and the spatial complexity is thus $O(1)$.

7. Simulation and Results

7.1. Simulation Settings. Three simulated environments were used for the performance analysis. In the following simulated environments, the distance between the sound source and the target is 7.5 km, the speed of the target is 14 m/s, the SNR = −10 dB, and the sample frequency $f_{sa} = 7000$ Hz. Here, the frequency band is denoted by F_s, and the pulse width is denoted by T_s.

Simulated environment 1: the HFM pulse sequences consist of the following HFM signals: for HFM signal 1, F_s is 200 Hz-1000 Hz, and the pulse width is 1 s. For HFM signal 2, F_s is 300 Hz-1200 Hz, and T_s is 2 s. For HFM signal 3, F_s is 400 Hz-1400 Hz, and T_s is 3 s. For HFM signal 4, F_s is 500 Hz-1600 Hz, and T_s is 4 s. For HFM signal 5, F_s is 600 Hz-1900 Hz, and T_s is 6 s.

Simulated environment 2: the HFM pulse sequences consist of the following HFM signals: for HFM signal 1, F_s is 100 Hz-200 Hz, and T_s is 1 s. For HFM signal 2, F_s is 700 Hz-900 Hz, and T_s is 2 s. For HFM signal 3, F_s is 1000 Hz-1200 Hz, and T_s is 3 s. For HFM signal 4, F_s is 1700 Hz-1900 Hz, and T_s is 4 s.

Simulated environment 3: the HFM pulse sequences consist of the following HFM signals: for HFM signal 1, F_s is 100 Hz-200 Hz, and T_s is 2 s. For HFM signal 2, F_s is

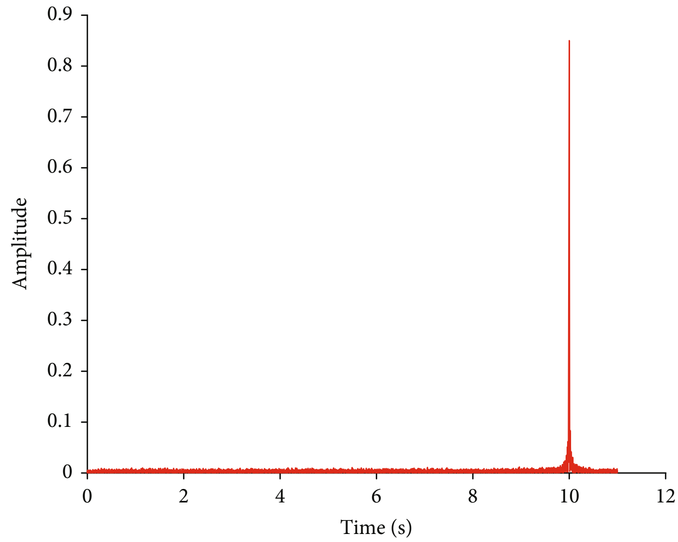

Figure 10: Pulse sequence method based on HFM signal under simulation environment 3.

Table 3: For simulated environment 3: comparison of simulation results.

(a)

Echo time of single signal (s) HFM signal 1	HFM signal 2	HFM signal 3	HFM signal 4	Ranging of single signal (km) HFM signal 1	HFM signal 2	HFM signal 3	HFM signal 4	Ranging of PHS (km)	Speed of PHS (m/s)
10.0754	9.8682	10.245	10.1224	7.55655	7.40115	7.68375	7.5918	7.5	13.996

(b)

Ranging error of PHS	Speed measurement error of PHS	Ranging error of single signal				Range accuracy improvement ratio compared to			
		HFM signal 1	HFM signal 2	HFM signal 3	HFM signal 4	HFM signal 1	HFM signal 2	HFM signal 3	HFM signal 4
0%	0.02857%	0.754%	1.318%	2.45%	1.224%	100%	100%	100%	100%

1000 Hz-700 Hz, and T_s is 3 s. For HFM signal 3, F_s is 1000 Hz-1300 Hz, and T_s is 3 s. For HFM signal 4, F_s is 1100 Hz-1300 Hz, and T_s is 1 s.

7.2. Simulation Results. For simulated environment 1, the performance analysis is shown in Figures 5 and 6. The numerical results of PHS are given in Table 1. From Figure 5, it can be seen that, after matched filtering, the signal echo time of HFM signal 1, HFM signal 2,HFM signal 3, HFM signal 4, and HFM signal 5 is 10.0236 s, 10.0502 s, 10.0792 s, 10.1096 s, and 10.1652 s, respectively. Figure 6 shows the MTD operation based on pulse sequence method. According to Equation (18), the value of v is 13.9914 m/s. It can be seen from Table 1 that the speed measurement error and the ranging error of PHS are 0.061429% and 0%, respectively. The ranging error of HFM signal 1, HFM signal 2, HFM signal 3, HFM signal 4, and HFM signal 5 is 0.0236%, 0.502%, 0.792%, 1.096%, and 1.652%, respectively. Compared with HFM signal 1, HFM signal 2, HFM signal 3, HFM signal 4, and HFM signal 5, the ranging measurement accuracy of PHS is all improved by 100%.

For simulated environment 2, the performance analysis is shown in Figures 7 and 8. The numerical results of PHS are given in Table 2. From Figure 7, it can be seen that, after matched filtering, the signal echo time of HFM signal 1, HFM signal 2, HFM signal 3, and HFM signal 4 is 10.0376 s, 10.1696 s, 10.3392 s, and 10.7160 s, respectively. Figure 8 shows the pulse sequence method based on HFM signals. According to Equation (18), the value of v is 14.0019 m/s. It can be seen from Table 2 that the speed measurement error and the ranging error of PHS are 0.013571429% and 0%, respectively. The ranging error of HFM signal 1, HFM signal 2, HFM signal 3, and HFM signal 4 is 0.376%, 1.696%, 3.392%, and 7.16%, respectively. Compared with HFM signal 1, HFM signal 2, HFM signal 3, and HFM signal 4, the ranging measurement accuracy of PHS is all improved by 100%.

For simulated environment 3, the performance analysis is shown in Figures 9 and 10. The numerical results of

PHS are given in Table 3. From Figure 9, it can be seen that, after matched filtering, the signal echo time of HFM signal 1, HFM signal 2,HFM signal 3, and HFM signal 4 is 10.0754 s, 9.8682 s, 10.245 s, and 10.1224 s, respectively. Figure 10 shows the pulse sequence method based on HFM signals. According to Equation (18), the value of v is 13.996 m/s. It can be seen from Table 3 that the speed measurement error and the ranging error of SPHS are 0.02857% and 0%, respectively. The ranging error of HFM signal 1, HFM signal 2, HFM signal 3, and HFM signal 4 is 0.754%, 1.318%, 2.45% and 1.224%, respectively. Compared with HFM signal 1, HFM signal 2, HFM signal 3, and HFM signal 4, the ranging measurement accuracy of PHS is all improved by 100%.

8. Conclusion

The fuzzy function of HFM signal has the shape of the blade, which makes the velocity and distance to be coupled together. Due to the Doppler frequency shift caused by the target movement, the peak value after the matched filtering has a time delay in the time domain, resulting in the failure of a single HFM to accurately range. In this paper, based on the time delay of signals with different frequency bands or different pulse widths, a pulse sequence method based on HFM for speed measurement (PHS) is proposed, which uses HFM signals of different frequency bands and pulse widths in the sequence. The proposed method can not only guarantee the speed measurement but also improve the accuracy of the speed measurement and distance measurement.

In future research, we will realize simulation in more complex scenarios, such as multitarget speed measurement and simulation in the presence of clutter.

Data Availability

The data used to support the findings of this study are restricted.

Conflicts of Interest

The authors declare that they have no conflicts of interest.

Acknowledgments

This work was supported in part by the Shandong Smart Ocean Ranch Engineering Technology Collaborative Innovation Center, in part by the Shandong Agricultural Science and Technology Service Project (No. 2019FW037-4), in part by the research fund for high-level talents of Qingdao Agricultural University (No. 6631119041), and in part by the Shandong Technology Innovation Guidance Program (No. 2020LYXZ023).

References

[1] Y. Zhu, *Principle of Active Sonar Detection Information*, Science press, 2014.

[2] T. Tan, *Sonar Technology*, Harbin Engineering University Press, Harbin, 2010.

[3] R. Diamant, A. Feuer, and L. Lampe, *Choosing the Right Signal: Doppler Shift Estimation for Underwater Acoustic Signals*, Acm International Conference on Underwater Networks & Systems, 2012.

[4] Z. Meng, J. J. Zhang, and A. Papandreou-Suppappola, “Hyperbolic Frequency Modulation for Multiple Users in Underwater Acoustic Communications,” in *2014 IEEE International Conference on Acoustics, Speech and Signal Processing (ICASSP)*, Florence, Italy, 2014.

[5] Y. Peng, C. Song, L. Qi et al., “Jlhs: a joint linear frequency modulation and hyperbolic frequency modulation approach for speed measurement,” *IEEE Access*, vol. 8, pp. 205316–205326, 2020.

[6] P. Liu and C. Song, “Sch: a speed measurement method of combined hyperbolic frequency modulation signals,” *IEEE Access*, vol. 9, pp. 95986–95993, 2021.

[7] J. Yang and T. K. Sarkar, “A new doppler-tolerant polyphase pulse compression codes based on hyperbolic frequency modulation,” in *2007 IEEE Radar Conference*, Waltham, MA, USA, 2007.

[8] S. V. Maric and E. L. Titlebaum, “A class of frequency hop codes with nearly ideal characteristics for use in multiple-access spread-spectrum communications and radar and sonar systems,” *IEEE Transactions on Communications*, vol. 40, no. 9, pp. 1442–1447, 1992.

[9] W. P. Whyland, “Doppler consistent hyperbolic frequency modulation,” *US Patent*, vol. 5, 1991.

[10] Z. Shao, T. Chen, and G. Wang, *A method of underwater moving target detection base on hfm and cw signals*, 2017 Western China Acoustics Academic Exchange Conference, 2017.

[11] F. Gini and G. B. Giannakis, “Parameter estimation of hybrid hyperbolic fm and polynomial phase signals using the multilag high-order ambiguity function,” in *Conference Record of the Thirty-First Asilomar Conference on Signals, Systems and Computers (Cat. No.97CB36136)*, pp. 250–254, Pacific Grove, CA, USA, 1997.

[12] M. Xin, *HFM acoustic preamble signal detection algorithm based on match filter and waveform design in underwater communication, [Ph.D. thesis]*, Harbin Institute of Technology, 2017.

[13] L. Zhang, X. Xu, W. Feng, and Y. Chen, “Hfm spread spectrum modulation scheme in shallow water acoustic channels,” in *2012 Oceans*, Hampton Roads, VA, USA, 2012.

[14] J. V. Suman and J. B. Seventline, “Separation of HFM and NLFM signals for radar using fractional Fourier transform,” in *2014 International Conference on Communication and Network Technologies*, Sivakasi, India, 2014.

[15] C. Liu, S. Liu, C. Zhang, Y. Huang, and H. Wang, “Multipath Propagation Analysis and Ghost Target Removal for FMCW Automotive Radars,” in *IET International Radar Conference (IET IRC 2020)*, Chongqing, China, 2020.

[16] J. J. Murray, “On the doppler bias of hyperbolic frequency modulation matched filter time of arrival estimates,” *IEEE Journal of Oceanic Engineering*, vol. 44, no. 2, pp. 446–450, 2019.

[17] Y. Chen, Y. Zhu, H. Zhao, and Q. Fu, “Detection algorithm reaseach of high velocity moving target based on the envelope interpolation,” *Signal Processing*, vol. 20, no. 4, pp. 387–390, 2004.